

Superconductivity in $\text{Ba}_2\text{Sn}_3\text{Sb}_6$ and SrSn_3Sb_4

Laura Deakin,^a Robert Lam,^a Frank Marsiglio,^b and Arthur Mar^{a,*}

^a *Department of Chemistry, University of Alberta, Edmonton, AB Canada T6G 2G2*

^b *Department of Physics, University of Alberta, Edmonton, AB Canada T6G 2J1*

* Corresponding author. Tel: (780) 492-5592. Fax: (780) 492-8231. E-mail: arthur.mar@ualberta.ca

Abstract

Resistivity and ac magnetic susceptibility measurements on $\text{Ba}_2\text{Sn}_3\text{Sb}_6$ and SrSn_3Sb_4 indicate that these Zintl compounds display a transition to a superconducting phase at $T_C = 3.9$ K. The Meissner effect was observed for $\text{Ba}_2\text{Sn}_3\text{Sb}_6$ under an applied field of 25 Oe. The signatures for superconductivity, such as high and low velocity conduction electrons and lone pairs, are present for both of these compounds.

Keywords: Antimonide; Zintl phase; Superconductivity

1. Introduction

Zintl compounds [1], consisting of an alkali or alkaline earth element combined with a p-block element, have generally been assumed to be semiconductors, despite the absence of experimental transport data in most cases. Where measurements have been made, the low-temperature data remain sparse. However, there is mounting evidence that challenges the assumption of semiconductivity, particularly in borderline Zintl compounds involving heavier p-block elements where the band gap can be narrowed considerably. For instance, some Zintl phases such as $\text{Ba}_8\text{In}_4\text{Sb}_{16}$ [2] and BaGa_2Sb_2 [3] are found to be narrow band gap p-type semiconductors, and a few such as $\text{Ba}_3\text{Sn}_4\text{As}_6$ are metallic [4]. Some binary borderline Zintl phases are superconducting, such as BaSn_3 ($T_C = 4.3 \text{ K}$)⁵ and SrSn_3 ($T_C = 5.4 \text{ K}$) [6]. The observation of superconductivity has been connected to the simultaneous presence of both high and low velocity conduction electrons in the band structure [7], the existence of van Hove singularities (saddle points) near E_F [8], and low dimensionality of the structure [9]. We aver that borderline metallic Zintl compounds are potentially a rich source of candidates displaying conventional superconductivity as both localized and itinerant electronic behaviour is often encountered, and their structures frequently display low-dimensional features in the anionic networks [10].

The ternary antimonides $\text{Ba}_2\text{Sn}_3\text{Sb}_6$ [11] and SrSn_3Sb_4 [12] are Zintl compounds that possess related channel structures made up of 30-membered rings in their Sn–Sb anionic frameworks (Figure 1). The channels run down the crystallographic b axis in both cases and accommodate the alkaline-earth cations. In $\text{Ba}_2\text{Sn}_3\text{Sb}_6$, zigzag Sb chains also reside within the channels. The resistivities were previously measured only down to 25 K and indicated metallic behaviour with an approach toward the origin in the case of $\text{Ba}_2\text{Sn}_3\text{Sb}_6$ [13]. This observation,

along with characteristic signatures of flat and wide hole-like bands in the electronic band structure [13], prompted us to re-examine the physical properties at lower temperatures previously inaccessible to us. We present here evidence for superconductivity in the ternary antimonides $\text{Ba}_2\text{Sn}_3\text{Sb}_6$ and SrSn_3Sb_4 .

2. Experimental

Single crystals of $\text{Ba}_2\text{Sn}_3\text{Sb}_6$ and SrSn_3Sb_4 were grown from Sn flux reactions as described previously [11, 12]. The products were characterized by powder X-ray diffraction patterns collected on an Enraf-Nonius FR552 Guinier camera ($\text{Cu K}\alpha_1$ radiation; Si standard) and by EDX (energy-dispersive X-ray) analysis on a Hitachi S-2700 scanning electron microscope.

Electrical resistivities were measured by standard four-probe techniques on a Quantum Design PPMS system equipped with an ac-transport controller (Model 7100). The current was 0.1 mA and the frequency was 16 Hz. The resistivity was measured along the needle axis (crystallographic b axis) of single crystals of $\text{Ba}_2\text{Sn}_3\text{Sb}_6$ and SrSn_3Sb_4 . The compositions of all crystals used in these measurements were confirmed by EDX analysis. $\text{Ba}_2\text{Sn}_3\text{Sb}_6$: Anal. Calcd. (mol %) Ba, 18; Sn, 27; Sb, 55. Found: Ba, 14(2); Sn, 33(2); Sb, 53(2). SrSn_3Sb_4 : Anal. Calcd. (mol %) Sr, 12; Sn, 38; Sb, 50. Found: Sr, 7(2); Sn, 41(2); Sb, 52(2). Critical temperatures were determined at the point at which the resistivity is 90% that of the normal value. The field dependence of the resistivity was measured upon warming the sample after it was cooled under zero-field conditions.

Magnetic measurements on $\text{Ba}_2\text{Sn}_3\text{Sb}_6$ were made with use of a Quantum Design PPMS 9T magnetometer/susceptometer. Ac susceptibility measurements under various dc fields were

made upon warming the sample after it was cooled under zero-field conditions using a frequency of 1000 Hz and a driving amplitude of 1.0 Oe. The purity of the $\text{Ba}_2\text{Sn}_3\text{Sb}_6$ powder susceptibility sample was determined by Guinier powder X-ray diffraction. No lines characteristic of elemental Sn were observed. Any Sn impurities would be present at a level less than the detection limit of powder X-ray diffraction, on the order of less than 5%.

3. Results and discussion

The resistivity of single crystals of $\text{Ba}_2\text{Sn}_3\text{Sb}_6$ and SrSn_3Sb_4 down to 2 K is shown in Figure 2. There is a sudden decrease in resistivity at $T_C = 3.9$ K for both compounds. With increasing applied field (insets in Figure 2), the critical temperatures shift systematically to lower values. At temperatures below T_C , there exists a residual resistivity, which is attributed to surface degradation of the crystals resulting from the treatment of 6M HCl used to remove excess Sn flux. A surface reaction forming an insulating layer would impede the resistivity from descending to zero.

The temperature dependence of the ac magnetic susceptibility in this low-temperature range confirmed superconductivity behaviour in $\text{Ba}_2\text{Sn}_3\text{Sb}_6$ (Figure 3a). The diamagnetic shielding (zero-field-cooled) and Meissner effect (field-cooled) were observed at 25 Oe, and these curves are superimposable. We have been unable to prepare a sufficiently pure sample of SrSn_3Sb_4 to measure its magnetic susceptibility. The values of T_C for $\text{Ba}_2\text{Sn}_3\text{Sb}_6$ and SrSn_3Sb_4 do not coincide with that for elemental Sn ($T_C = 3.722$ K) [14]. Measurements of χ'_{ac} for elemental Sn (Cerac, 99.8 %) and $\text{Ba}_2\text{Sn}_3\text{Sb}_6$ under identical instrumental conditions (Figure 3b) confirmed that $\text{Ba}_2\text{Sn}_3\text{Sb}_6$ displays a T_C value that is noticeably different. Moreover, the use of single crystals, previously screened by EDX analyses, for the resistivity measurements precludes

the possibility that the superconductivity arises from elemental Sn.

The appearance of superconductivity in $\text{Ba}_2\text{Sn}_3\text{Sb}_6$ and SrSn_3Sb_4 is consistent with the presence of disperse bands crossing the Fermi level and flat bands near the Fermi level in the band structure [13]. The disperse bands arise from orbital interactions oriented along the channel directions; the flat bands, perpendicular to them. The lone pairs associated with SnSb_3 trigonal pyramids in the crystal structures of both compounds may also be significant. There have been recent suggestions implicating a correlation between superconductivity and the presence of lone pairs in metallic conductors [5, 8]. We note that in a previous study, the ternary antimonide $\text{La}_{13}\text{Ga}_8\text{Sb}_{21}$, containing pyramidally distorted GaSb_3 units, is a superconductor ($T_C = 2.4$ K), whereas the related compound $\text{La}_{12}\text{Ga}_4\text{Sb}_{23}$, containing planar GaSb_3 units, is a normal metal [15]. Another suggestion is that the hole-like nature of the bands crossing the Fermi level may be significant for superconductivity [16, 17]. This theory can be tested by attempting to dope these compounds with holes and electrons, with the result that T_C as a function of doping concentration will exhibit a familiar bell-shaped curve.

Low-temperature physical property measurements on EuSn_3Sb_4 , isostructural with SrSn_3Sb_4 but containing unpaired $4f$ electrons, are currently being undertaken. More rigorous electronic structure calculations may also prove helpful.

Acknowledgments

The Natural Sciences and Engineering Research Council of Canada and the University of Alberta supported this work. We thank Wing Yan Chan for assistance with the preparation of $\text{Ba}_2\text{Sn}_3\text{Sb}_6$, and Christina Barker (Department of Chemical and Materials Engineering) for assistance with the EDX analyses.

References

- [1] S. M. Kauzlarich (Ed.), Chemistry, Structure and Bonding of Zintl Phases and Ions, VCH Publishers, New York, 1996.
- [2] S.-J. Kim, S. Hu, C. Uher, M. G. Kanatzidis, Chem. Mater. 11 (1999) 3154.
- [3] S.-J. Kim, M. G. Kanatzidis, Inorg. Chem. 40 (2001) 3781.
- [4] R. Lam, A. Mar, Solid State Sciences 3 (2001) 503 and references therein.
- [5] T. F. Fässler, C. Kronseder, Angew. Chem. Int. Ed. Engl. 36 (1997) 2683.
- [6] T. F. Fässler, S. Hoffmann, Z. Anorg. Allg. Chem. 626 (2000) 106.
- [7] C. Fesler, J. Solid State Chem. 160 (2001) 93.
- [8] A. Simon, Angew. Chem. Int. Ed. Engl. 36 (1997) 1788.
- [9] R. B. King, J. Chem. Inf. Comput. Sci. 39 (1999) 180.
- [10] G. A. Papoian, R. Hoffmann, Angew. Chem. Int. Ed. 39 (2000) 2408.
- [11] R. Lam, A. Mar, Inorg. Chem. 35 (1996) 6959.
- [12] D. T. Chow, R. McDonald, A. Mar, Inorg. Chem. 36 (1997) 3750.
- [13] R. Lam, J. Zhang, A. Mar, J. Solid State Chem. 150 (2000) 371.
- [14] B. W. Roberts, Properties of Selected Superconductive Materials, US Government Printing Office, Washington, DC, 1978.
- [15] A. M. Mills, L. Deakin, A. Mar, Chem. Mater. 13 (2001) 1778.
- [16] J. E. Hirsch, Phys. Lett. A 134 (1989) 451.
- [17] J. E. Hirsch, F. Marsiglio, Phys. Rev. B 39 (1989) 11515.

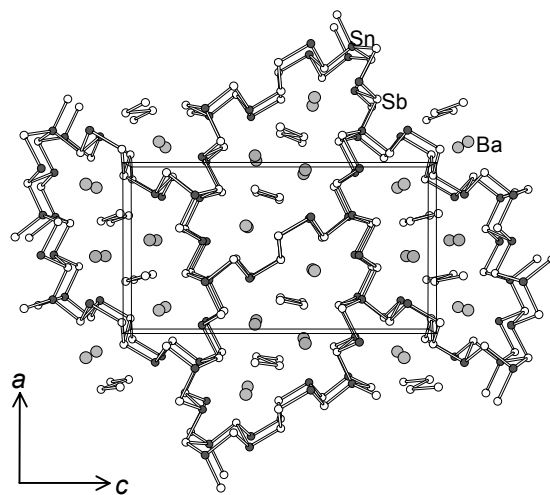
Figure captions

Fig. 1. Structures of (a) $\text{Ba}_2\text{Sn}_3\text{Sb}_6$ and (b) SrSn_3Sb_4 viewed down the b axis. The large lightly-shaded circles are Ba or Sr atoms, the solid circles are Sn atoms, and the open circles are Sb atoms.

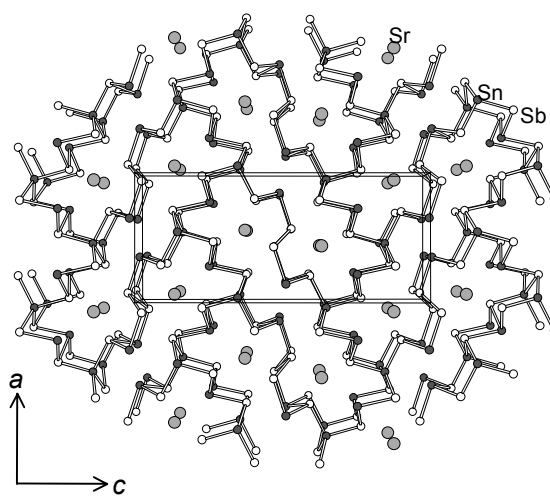
Fig. 2. Resistivity of (a) $\text{Ba}_2\text{Sn}_3\text{Sb}_6$ and (b) SrSn_3Sb_4 . Insets show the field dependence of the resistivity between 0 and 500 Oe. Lines are included to guide the eye.

Fig. 3. (a) Field dependence of the zero-field-cooled ac magnetic susceptibility of $\text{Ba}_2\text{Sn}_3\text{Sb}_6$ and the field-cooled susceptibility acquired under a 25 Oe applied dc field. (b) Normalized ac magnetic susceptibilities of $\text{Ba}_2\text{Sn}_3\text{Sb}_6$ and elemental Sn under a zero dc field.

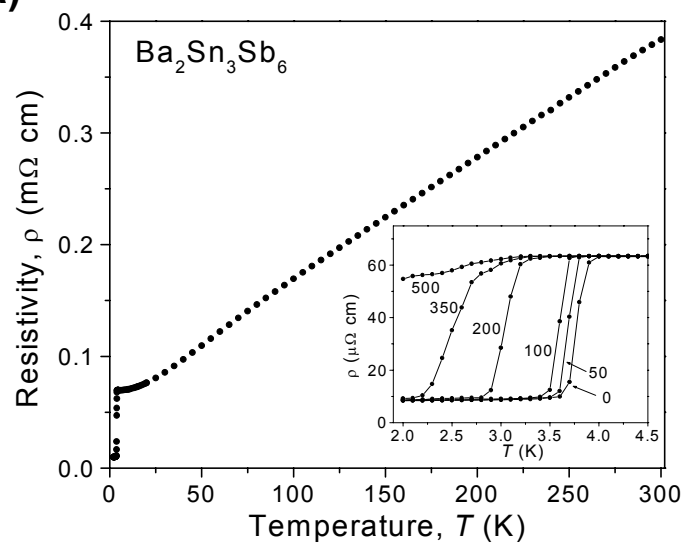
(a)



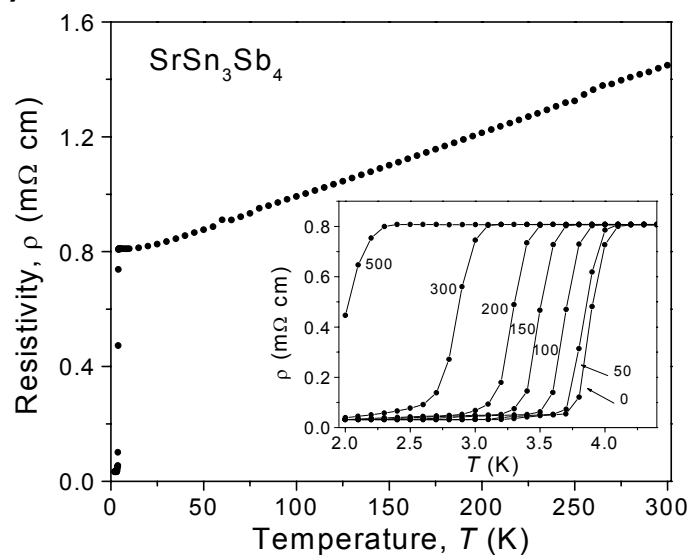
(b)

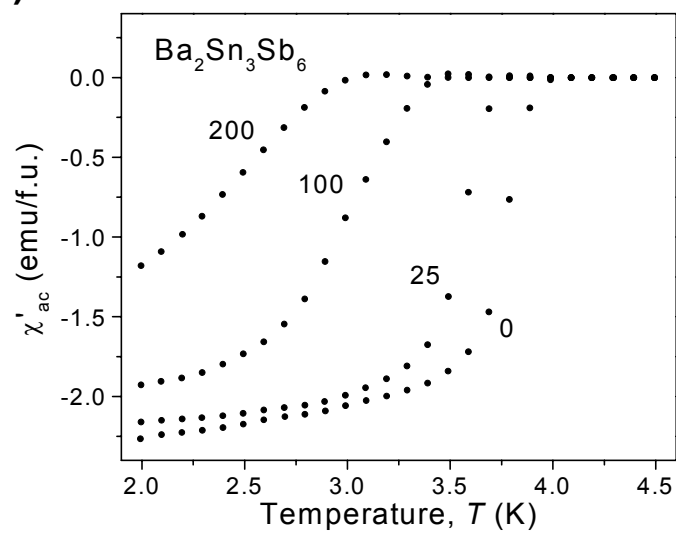


(a)



(b)



(a)**(b)**